Swelling Behavior and Structural Characteristics of Polyvinyl Alcohol/Montmorillonite Nanocomposite Hydrogels

M. Sirousazar,[1] M. Kokabi,[1] Z. M. Hassan[2]

[1]*Polymer Engineering Department, Faculty of Chemical Engineering, Tarbiat Modares University, Tehran, I.R. Iran*
[2]*Immunology Group, Faculty of Medical Science, Tarbiat Modares University, Tehran, I.R. Iran*

Received 21 October 2009; accepted 27 February 2011
DOI 10.1002/app.34437
Published online 25 July 2011 in Wiley Online Library (wileyonlinelibrary.com).

ABSTRACT: A series of nanocomposite hydrogels based on polyvinyl alcohol containing 0–10 wt % of the organically modified montmorillonite clay were prepared by freezing-thawing cyclic method. The morphology of the nanocomposite hydrogels was observed by the scanning electron microscopy technique. The structural properties were determined by measuring the network mesh size, crosslinking density, and average molecular weight of polymer chains between crosslinks. The swelling behavior and the effect of swelling medium temperature on the swelling kinetics and characteristics of the nanocomposite hydrogels were also investigated. The results showed that two structural characteristics i.e., network mesh size and average molecular weight of polymer chains between crosslinks have inverse dependence on the clay loading level in the nanocomposite hydrogel, while crosslinking density shows completely direct dependence. Swelling measurements demonstrated a linear relation between the degree of swelling and the square root of immersion time at all swelling medium temperatures. The results indicated that the swelling characteristics of the nanocomposite hydrogels including the equilibrium degree of weight and volume swelling and the equilibrium water content were decreased by increasing the quantity of the clay incorporated into the hydrogel as well as by decreasing the temperature of swelling medium. While, the time required to reach to the equilibrium condition, as another swelling characteristic of the hydrogels, exhibited a completely opposite behavior. © 2011 Wiley Periodicals, Inc. J Appl Polym Sci 123: 50–58, 2012

Key words: nanocomposites; hydrogels; swelling; polyvinyl alcohol; montmorillonite

INTRODUCTION

Hydrogels are crosslinked three-dimensional hydrophilic polymer networks capable of uptaking and holding large amounts of water or aqueous solutions while maintaining the structure.[1] They have attracted many scientific attentions as soft materials and demonstrated excellent potential in numerous applications, such as superabsorbents,[2] molecular filtration,[3] separation and bio-separation processes.[4,5] In biomedical field, their usages are included implants,[6] artificial organs,[7] contact lenses,[8] and wound dressings.[9,10] They have also gained wide pharmaceutical applications as drug delivery devices.[11,12] However, the practical application of the conventional polymer hydrogels is restricted because of their weak mechanical properties e.g., low gel strength, poor stability, and low fracture toughness.[13–16] These disadvantages are mainly attributed to the restricted molecular motion of the polymer chains due to the large number of randomly arranged crosslinks in the conventional hydrogels.[17] Therefore, improvement of the mechanical properties of the polymer hydrogels is necessary to extend their applications.

Since 2002, several attempts have been made to reinforce the structure of hydrogels by incorporating the nanoparticles or nanostructures to them to obtain the nanocomposite hydrogels with enhanced mechanical, physical, and chemical properties.[18,19] In the past years, most researches on the nanocomposite hydrogels have been focused on the use of clays such as laponite,[20–25] montmorillonite,[26–30] hydrotalcite,[31–33] and bentonite[34] as nanoparticles. Furthermore, some nanocomposite hydrogels have been prepared using the other types of nanoparticles e.g., silver[35,36] and iron oxide (Fe_3O_4)[37] particles. We have previously prepared nanocomposite hydrogels based on polyvinyl alcohol (PVA) and organically modified montmorillonite (OMONT) using freezing-thawing method and investigated their potentials as novel wound dressing devices.[38,39] Freezing-thawing is a physical method to produce the PVA hydrogel. It is a simple method of crosslinking which does not require any additional chemicals and high temperature. PVA hydrogels obtained by repeated freezing-

Correspondence to: M. Kokabi (mehrir@modares.ac.ir).
Contract grant sponsor: Tarbiat Modares University.

thawing process are non toxic and strong which have demonstrated a great potential for various applications.[40,41]

Reviewing the literatures on the nanocomposite hydrogels shows that numerous research studies have been performed on those nanocomposite hydrogels which their crosslinking process is done mainly via using chemical crosslinking agents (so-called as chemical nanocomposite hydrogels). While nearly no essential attentions have been paid to the nanocomposite hydrogels crosslinked physically in the absence of chemical crosslinking agents, like those which can be prepared via freezing-thawing technique.

In this work, the PVA nanocomposite hydrogels were prepared via a physical crosslinking method (i.e., freezing-thawing cyclic technique) using OMONT as nanoparticle. The effect of clay on some network properties and structural characteristics of the PVA hydrogel was studied. The swelling behavior of the prepared nanocomposite hydrogels was investigated as well. The effect of medium temperature on the swelling kinetics and characteristics of these nanocomposite hydrogels was also studied.

EXPERIMENTAL

Materials

All experiments utilized commercial grade PVA having a degree of polymerization of 1700 and a saponification value of greater than 98%, was purchased from the Nippon Synthetic Chemical Industry, Japan. Montmorillonite (MONT) was supplied by Zhejiang Fenghong Clay Chemicals, P.R. China. This clay has exchangeable sodium ions, and a cation exchange capacity of about 100 meq/100 g. Cetyltrimethylammonium bromide (CTAB) was supplied by Dishman Pharmaceuticals and Chemicals, India. Double distilled water (DDW) was used to prepare all aqueous solutions.

Preparation of nanocomposite hydrogels

The organically modification of MONT to obtain OMONT was performed by using CTAB as reported elsewhere.[38] PVA-OMONT nanocomposite hydrogels containing 15 wt % of PVA and 0, 2, 5, 7, and 10 wt % of OMONT (based on PVA mass) were also prepared via the freezing-thawing cyclic method according to the procedure mentioned in our previous work.[38]

Scanning electron microscopy (SEM)

SEM technique was used to investigate the morphology of the prepared hydrogels. For this purpose, the hydrogels containing 0 and 5 wt % of clay were frozen in liquid nitrogen and then freeze dried at -40°C for 4 h until all water had sublimed. Cross sections of the freeze dried hydrogels were coated with gold. The morphology of samples was observed using a scanning electron microscope (Philips XL30, Netherlands).

Tensile test

The tensile test was accomplished to determine some mechanical and structural characteristics of the nanocomposite hydrogels including the tensile modulus, average molecular weight of PVA chains between crosslinks ($\overline{M}_c$), crosslinking density (ν_e), and also network mesh size (ξ). Three individual pieces of each hydrogel were cut into dumbbell shape samples with a thickness of 3 mm according to ASTM D-1822-L. Measurements were performed by recording the stress-strain data of samples using a 5 tons tensiometer (Pars Paygir, Iran) with a constant crosshead speed of 100 mm min^{-1} at room temperature (25°C).

The network and structural characteristics of hydrogels were calculated on the basis of the theory of rubber elasticity using the obtained stress (τ) and stretching ratio (α) data. In previous works, the theory of rubber elasticity has been used successfully for nanocomposite hydrogel.[17,24,25,42,43] ($\overline{M}_c$) was calculated as a function of the slop of the linear region of curve τ versus $\left(\alpha - \frac{1}{\alpha^2}\right)$ for each hydrogel using the following equation:[44]

$$\tau = \frac{\rho RT}{\bar{M}_c}\left[1 - \frac{2\bar{M}_c}{\bar{M}_n}\right]\left(\alpha - \frac{1}{\alpha^2}\right) \quad (1)$$

where ρ, ($\overline{M}_n$), and T are density and molecular weight of PVA, and test temperature, respectively. ξ was also calculated using the eq. (2):[44]

$$\xi = \nu_p^{-1/3} l\left[C_n\left(\frac{2\bar{M}_c}{M_r}\right)\right]^{1/2} \quad (2)$$

where ν_p and M_r are the volume fraction of PVA in hydrogel and the molecular weight of the repeating unit of the polymer chain, respectively. While, l, C_n, and R are the carbon–carbon bond length (1.54 Å), the Flory characteristic ratio (8.3 for PVA) and the gas constant, respectively. The crosslinking densities of the hydrogels were calculated based on the following equation:[45]

$$\nu_e = \frac{\rho}{\bar{M}_c}\left(1 - \frac{2\bar{M}_c}{\bar{M}_n}\right) \quad (3)$$

Gel fraction

To perform the gel fraction measurements, three preweighed slices of each sample were dried under vacuum at room temperature until observing no change in their weights. Nearly identical weights of other slices of the same sample were immersed into the excess of DDW for 4 days to remove uncrosslinked species. Subsequently, the immersed samples were separated from DDW and dried at room temperature under vacuum until the dried samples showed constant weights.

The gel fraction of the hydrogels was calculated on the basis of the weight ratio of dried samples in rinsed and unrinsed conditions as follows:

$$\text{Gel fraction}\,(\%) = \frac{W_f - W_c}{W_i - W_c} \times 100 \qquad (4)$$

where, W_f and W_i are the weights of the dried hydrogel after and before rinsing and extraction, respectively, and W_c is the weight of organoclay incorporated into the sample. The average value of three experiments was reported as the final gel fraction value for each sample.

Swelling measurements

Swelling kinetics and characteristics of PVA nanocomposite hydrogels were obtained by measuring their initial and swollen weights in DDW at various temperatures and time intervals. Approximately 1 g of each completely extracted and dried samples were weighed and their volume measured and then immersed into 500 ml of DDW. At desired time intervals, swollen samples were removed from DDW and weighed after gentle surface wiping by absorbent paper. Swelling experiments were performed at 20, 37, and 50°C in thermostatically controlled water bath and data recording continued until reaching a constant weight value. The final volume of samples, i.e., volume at equilibrium condition, was also measured as equilibrium swelling characteristics of the hydrogels.

The degree of swelling which is defined as the ratio of the water weight for swollen gel to the weight of dried gel, was calculated as a criterion of swelling kinetics of samples according to eq. (5).

$$\text{Degree of swelling}\,(\%) = \frac{W_s(t) - W_d}{W_d} \times 100 \qquad (5)$$

where W_d is the final weight of the dried sample and $W_s(t)$ is the weight of the same swelled sample at a specified immersion time interval (t).

The equilibrium swelling characteristics including equilibrium degree of weight swelling (EDWS), equilibrium water content (EWC), and equilibrium degree of volume swelling (EDVS) were also calculated by eqs. (6)–(8), respectively.

$$\text{EDWS}\,(\%) = \frac{W_{se} - W_d}{W_d} \times 100 \qquad (6)$$

$$\text{EWC}\,(\%) = \frac{W_{se} - W_d}{W_{se}} \times 100 \qquad (7)$$

$$\text{EDVS}\,(\%) = \frac{V_{se} - V_d}{V_d} \times 100 \qquad (8)$$

where W_{se} and V_{se} are the swollen weight and volume of the sample at equilibrium condition, respectively, and V_d is the final volume of the extracted and dried sample. All swelling measurements were repeated three times for each sample.

RESULTS AND DISCUSSION

Morphology and structural characteristics

In our previous study,[38] the X-ray diffraction (XRD) and transmission electron microscopy (TEM) methods were used to determine the morphology of the PVA-OMONT nanocomposite hydrogels. The results showed an increase in the d-spacing of OMONT in the presence of PVA, implying that the PVA without any serious dependence on the OMONT loading has intercalated between individual silicate layers during the freezing-thawing process.

In this work, morphology of the prepared hydrogels was observed by SEM and their structural characteristics, i.e., $(\overline{M}_c)$, ν_e, and ξ were determined using the tensile test. The SEM micrographs of the clay-free PVA hydrogel and 5 wt % OMONT loaded nanocomposite hydrogel are shown in Figure 1. It is seen that the apparent micro-scale pore size decreases with incorporating clay to the PVA hydrogel. Although this may be attributed to the presence of the clay in the PVA hydrogel matrix and its action as additional crosslinkers which may create more densely crosslinked network with smaller pore size, but it would be better to reach to this conclusion based on the calculated structural characteristics of the PVA-OMONT nanocomposite hydrogels.

In Figure 2, representative curves showing the fitting of eq. (1) were demonstrated by plotting τ versus $\left(\alpha - \frac{1}{\alpha^2}\right)$ for typical hydrogels. Excellent linear trends were found in the linear stretching region ($\alpha < 1.1$) for all samples. Figure 3 shows the tensile modulus values for PVA and PVA-OMONT nanocomposite hydrogels. It can be seen that incorporating OMONT to PVA increases the amount of tensile modulus and reinforces the hydrogel network. For instance, the tensile modulus of PVA nanocomposite

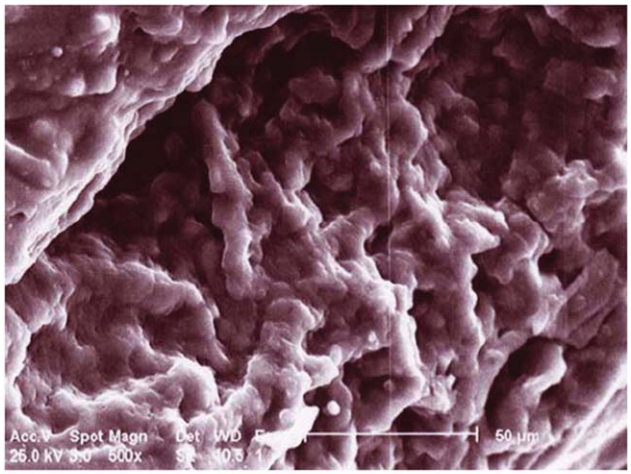

Figure 1 SEM micrographs of the (a) PVA hydrogel and (b) 5 wt % OMONT loaded nanocomposite hydrogel. [Color figure can be viewed in the online issue, which is available at wileyonlinelibrary.com.]

hydrogel containing 5 wt % OMONT is 1.2 times greater than of PVA hydrogel.

The effect of clay on $(\overline{M}_c)$ and ν_e of PVA-OMONT nanocomposite hydrogels is shown in Figure 4. It

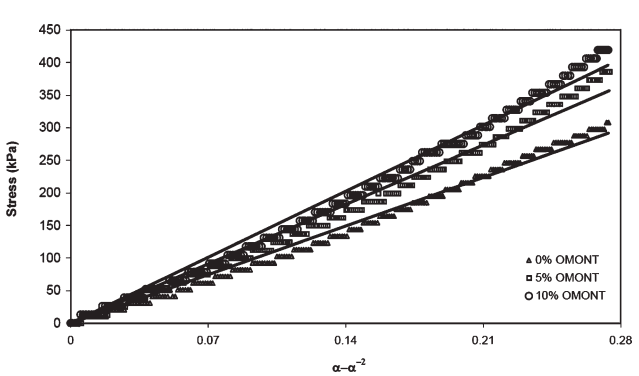

Figure 2 Typical stress-strain curves of samples.

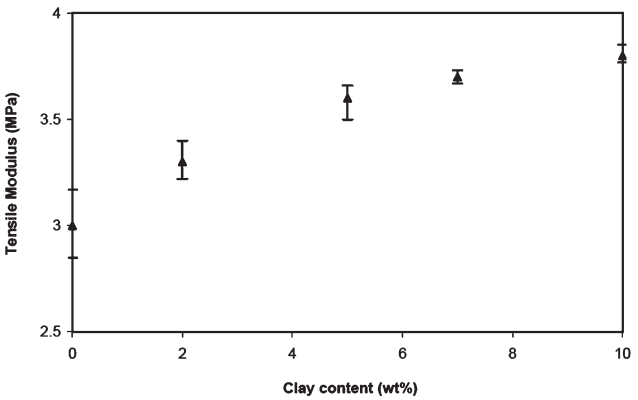

Figure 3 Tensile modulus of PVA-OMONT nanocomposite hydrogels.

can be observed that by adding OMONT to the PVA hydrogel the amount of $(\overline{M}_c)$ and ν_e have been decreased and increased, respectively. Figure 4 also demonstrates that any increase in the clay content lowers the amount of $(\overline{M}_c)$ and increases the value of ν_e as well. Increasing the amount of crosslinking density simply means that the number of crosslinkings or junction points per volume of PVA network has been increased by adding OMONT into it, which clearly poses the role of OMONT layers as additional crosslinking agents in the PVA-OMONT nanocomposite hydrogels. On the other word, the results reveal that incorporating the OMONT organoclay to PVA hydrogel results in a more entangled and crosslinked network.

Figure 5 demonstrates the effect of clay on the network mesh sizes of the PVA-OMONT nanocomposite hydrogels. As seen, any increscent in OMONT loading level leads to some decrease in the network mesh size of nanocomposite hydrogels. This is in accordance with the results achieved for the crosslinking density and means that the available free volume for the transport of the matters is reduced by incorporating the OMONT to the PVA matrix, because of increasing its crosslinking density.

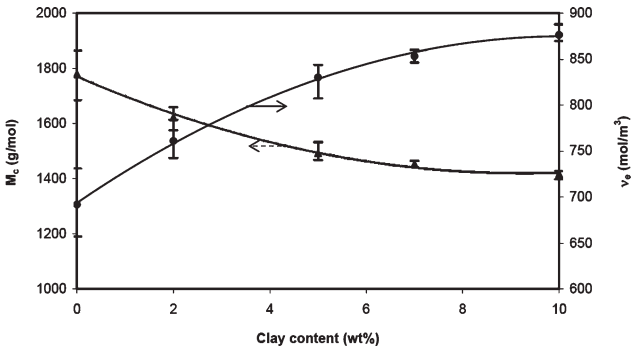

Figure 4 The effect of OMONT on the structural characteristics of PVA nanocomposite hydrogels.

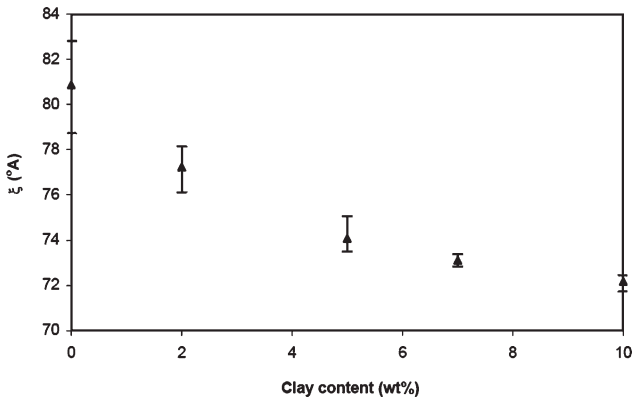

Figure 5 The network mesh sizes of the PVA-OMONT nanocomposite hydrogels.

Gel fraction

The gel fraction of prepared hydrogels and its dependence on the clay content is given in Figure 6. It can be seen that the gel fraction of samples is increased by increasing the content of clay from 0 up to 10 wt %. The gel fraction data reveal that the presence of clay within the three-dimensional network of hydrogel increases the number of cross-linked PVA chains, thus creates more entangled structure. The results indicate that when OMONT is added to the PVA hydrogel, some interactions are developed between functional groups of organoclay and those of the PVA chains. These additional interactions between PVA and OMONT, besides the bonds existed between PVA long neighboring chains due to crystallization, cause an increase in gel fraction value of the nanocomposite hydrogel. The gel fraction results are in a good agreement with the previously obtained results for the structural characteristics ($(\overline{M}_c)$, ν_e, and ξ).

Swelling of PVA nanocomposite hydrogels

As the structural characteristics and gel fraction values of the nanocomposite hydrogels change by varying the organoclay loading content, it is expected that their swelling characteristics and kinetics have been strongly affected by the amount of clay.

Figure 7 shows the degree of swelling versus the square root of immersion time for some typical samples (0, 5, and 10 wt % clay) at 37°C. It can be observed that an excellent linear correlation exists between the degree of swelling and the square root of immersion time for pure and nanocomposite hydrogels in early stages of swelling period. Similar observations have been reported by Urushizaki et al. for pure PVA hydrogels with different numbers of freezing-thawing cycles.[46] Figure 7 reveals that the swelling kinetics of PVA hydrogel does not alter due to presence of OMONT. And in general, the swelling kinetics of both PVA-OMONT nanocomposite hydrogels and pure PVA hydrogels obeys the diffusion-controlled mechanism. However, it can be seen that the degree of swelling consistently decreases by increasing the amount of clay in the samples. This is related to the network structure and gel fraction values of hydrogels, where the hydrogel has more entangled structure and higher gel fraction thus, has less capability of water uptaking and less degree of swelling.

Linear slopes of the degree of swelling versus square root of immersion time curves in Figure 7 are assumed to represent the relative swelling rate coefficient (SRC) of hydrogels. The SRC of hydrogels was calculated by dividing the slop values in Figure 7 by 100. The relationship between calculated SRC values and the gel fraction of pure and nanocomposite hydrogels were shown in Figure 8. Excellent linear relation between the gel fraction and SRC values is seen in the Figure 8. So, a linear equation can be used to express the swelling kinetics of PVA-OMONT nanocomposite hydrogels, as follows:

$$\mathrm{SRC} = a - b \times (\mathrm{Gel\,fraction}) \tag{9}$$

where a and b are constants which their values depend on some parameters such as PVA and clay properties and also processing parameters like the

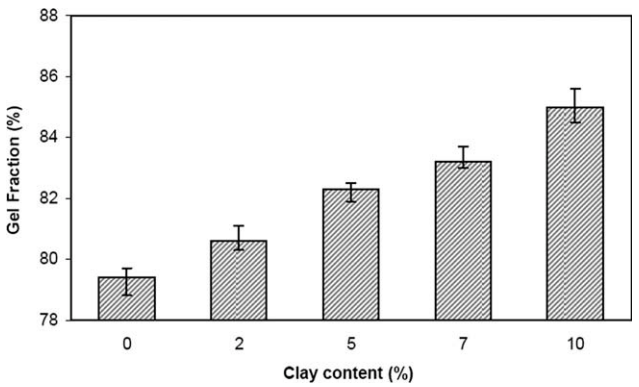

Figure 6 Gel fraction of PVA nanocomposite hydrogels.

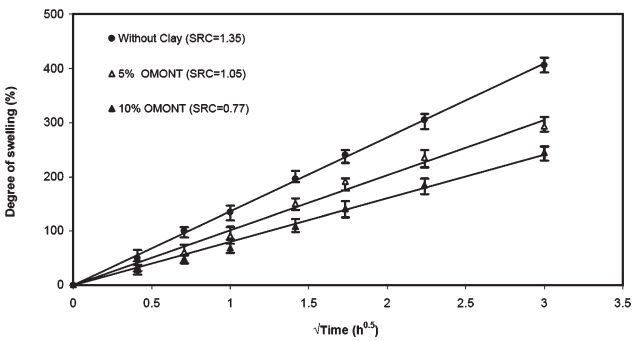

Figure 7 Degree of swelling versus square root of immersion time for some typical hydrogels.

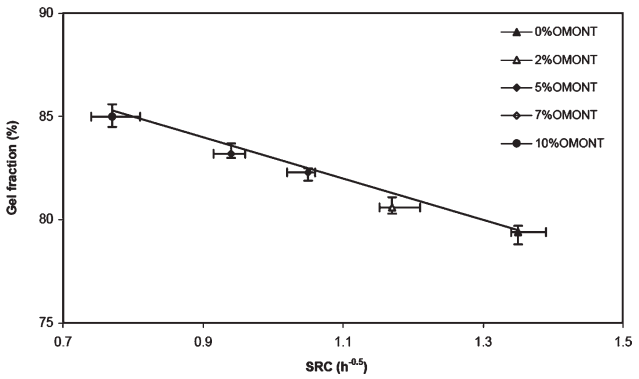

Figure 8 Gel fraction curve versus SRC of hydrogels.

number and temperature of freezing and thawing cycles and so on. Parameter *a* expresses the unachievable maximum value of SRC for the nanocomposite hydrogels and the parameter *b* states the intensity of dependence of SRC to the gel fraction value of hydrogel and also gives the decreasing rate of SRC with increasing the gel fraction amount. For the PVA-OMONT nanocomposite hydrogels prepared in this study (at swelling medium temperature of 37°C), the average values of *a* and *b* are 9.3 and 0.1 ($h^{-0.5}$), respectively.

Swelling characteristics of hydrogels at equilibrium condition including EDWS and EDVS, EWC and the time required to reach to the equilibrium state versus the value of organoclay added into PVA matrix are shown in Figures 9 and 10, respectively. Figures 9 and 10 demonstrate nearly similar trends for EDWS, EDVS, and EWC by increasing the value of organoclay loading level in hydrogels. It can be observed that there is an inverse relation between these parameters and OMONT loading level. The less values of these parameters for nanocomposite hydrogels in comparison to the pure hydrogel is related to their higher gel fraction values and more entangled structure as well as higher values of ν_e, which restricts the network relaxation and decreases the water uptake potential. On the other hand, a direct relation exists between the time required to reach to the equilibrium condition and organoclay loading level in hydrogels. Figure 10 shows that neat hydrogel has the least time required to reach to the equilibrium state and by increasing the quantity of OMONT, its value is increased, e.g., by adding only 5 wt % of OMONT an increment of 75% could be observed. The results indicate that the PVA nanocomposite hydrogels despite having less capability in water uptaking and swelling at equilibrium condition in comparison with pure PVA hydrogel, exhibit a slow swelling process with prolonged duration. The slower swelling of nanocomposite hydrogels can be attributed to the slower and more prolonged mass transfer process of the medium solution (water molecules) in the hydrogel network, which may be explained from two different views. First, as mentioned before, the crosslinking density of the hydrogel is increased by adding clay into it and its corresponding network mesh size also decreased. So, it is clear that some additional controlling steps against diffusion of molecules is created in nanocomposite hydrogel which may prolong the transport of molecules inside the network and as a result prolongs the swelling processes. Second, the layers of clay inside the nanocomposite hydrogel network act as physical barrier against molecules transport due to creating more tortuous paths which offers other controlling steps against mass transfer as well as swelling process. So, it can be remarked that the nanocomposite hydrogel needs more time to reach a specified level of swelling and therefore, shows slower swelling kinetics compared to clay-free hydrogel.

It seems that the nanocomposite hydrogels are suitable candidates for some practical applications where the swelling of hydrogel should be prolonged, e.g., in some drug delivery systems.

Temperature-dependent swelling behavior

To investigate the effect of medium temperature on swelling kinetics and characteristics of PVA-

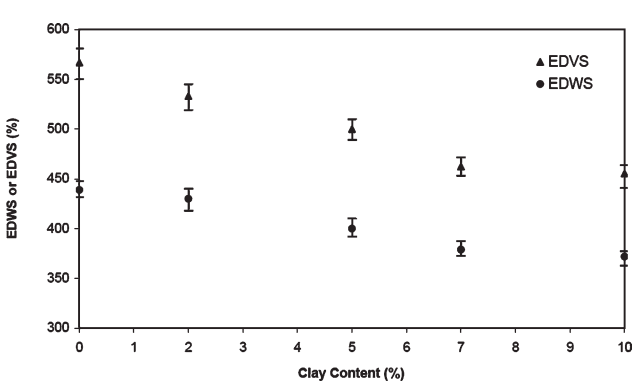

Figure 9 Equilibrium degree of weight and volume swelling versus clay content.

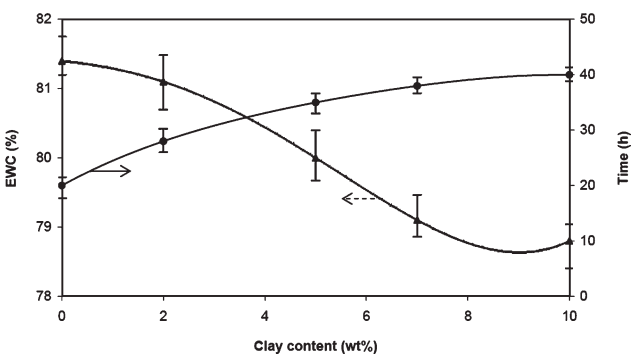

Figure 10 Equilibrium water content and the time required to reach equilibrium condition versus clay content.

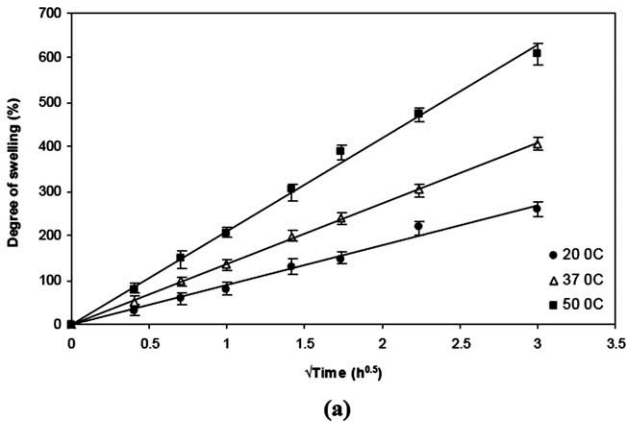

(a)

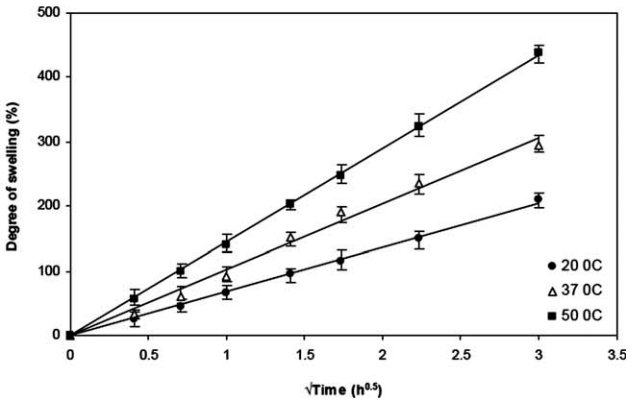

(b)

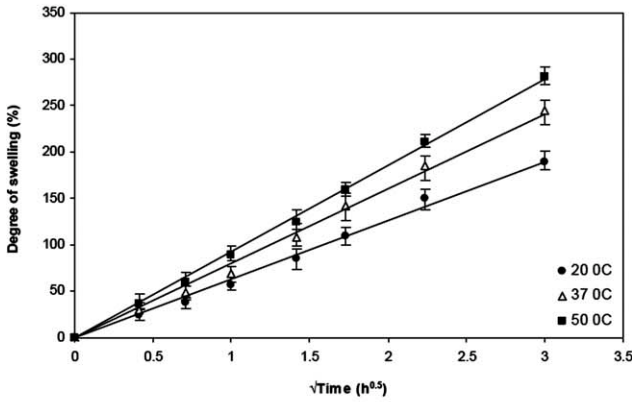

(c)

Figure 11 Degree of swelling against square root of immersion time at different temperatures for samples containing (a) 0 wt %, (b) 5 wt %, and (c) 10 wt % of OMONT.

OMONT nanocomposite hydrogels, the swelling experiments were repeated for some typical samples (hydrogels containing 0, 5, and 10 wt %) at 20 and 50°C. Figure 11 presents the degree of swelling curves against the square root of immersion time for pure hydrogel and nanocomposite hydrogels containing 5 and 10 wt % organoclay at various swelling temperatures. A linear relationship is observed between the degree of swelling and square root of

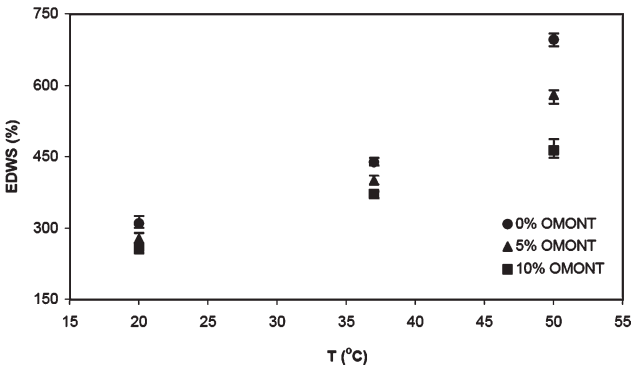

Figure 12 Equilibrium degree of weight swelling of hydrogels at different swelling temperatures.

immersion time at various temperatures for all of the samples. It means that the swelling kinetics of PVA hydrogels is independent of medium temperature and can be expressed by diffusion-controlled mechanism. However, increasing the medium temperature leads to an increase in the degree of swelling of hydrogels for all periods of immersion time. As Figure 11 shows, all the SRCs (the slopes of curves in Fig. 11) are affected by the swelling medium temperature. At higher temperatures, the hydrogel can uptake more water and poses higher SRC value.

Swelling characteristics at equilibrium conditions, i.e., EDWS, EWC, EDVS, and time required to reach to the equilibrium state were also determined at 20 and 50°C and the effect of temperature on them was investigated as well. Figures 12–14 show that the EDWS, EWC, and EDVS for samples containing 0, 5, and 10 wt % of organoclay at various temperatures, respectively. Similar to pure PVA hydrogel, the EDWS, EWC, and EDVS of PVA-OMONT nanocomposite hydrogels are increased by increasing the medium temperature. Figures 12–14 also show that the differences between these three characteristics of hydrogels at various organoclay loading levels are increased by increasing the swelling medium

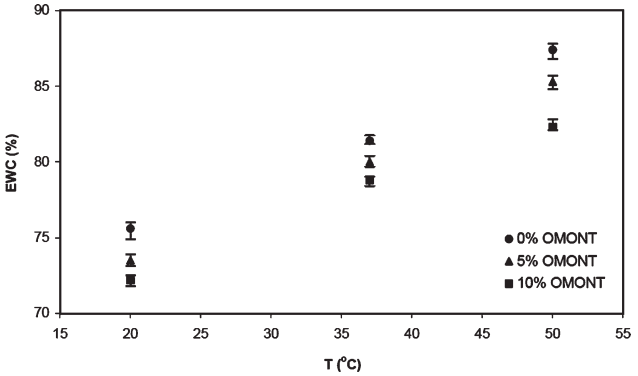

Figure 13 Equilibrium water content of hydrogels at different swelling temperatures.

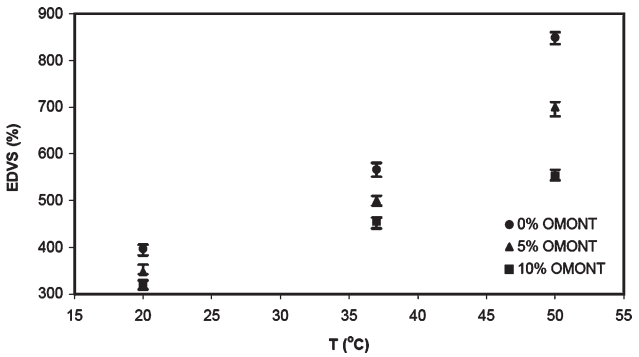

Figure 14 Equilibrium degree of volume swelling of hydrogels at different swelling temperatures.

temperature. For instance, the EDWS of pure hydrogel at 37°C is 1.18-fold greater than that of the nanocomposite hydrogel containing 10 wt % of OMONT, while this ratio at 50°C is 1.5 fold. This may be attributed to the decrease of the Flory polymer–solvent interaction parameter as well as increase of the polymer chains flexibility by increasing the swelling medium temperature.

In Figure 15 the curves of the times required to reach to the equilibrium state versus medium temperature were plotted for pure and some nanocomposite hydrogels. Increasing the temperature causes a decrease in the required time for reaching to the equilibrium condition in all samples. It means that pure and nanocomposite PVA hydrogels reach faster to the equilibrium swelling level at higher medium temperatures.

To show the influence of medium temperature on swelling behavior of PVA hydrogels and to achieve an appropriate mathematical relation to depict the affiliation of their swelling characteristics to temperature, the SRCs of the samples were plotted against medium temperature. For this purpose, the SRC of samples containing 0, 5, and 10 wt % of OMONT were calculated by deriving the slopes of their plots from Figure 11 and dividing them by 100. Then, an

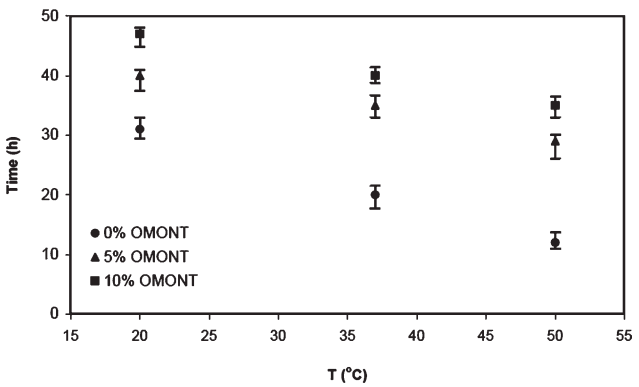

Figure 15 The time required to reach equilibrium condition of hydrogels at different swelling temperatures.

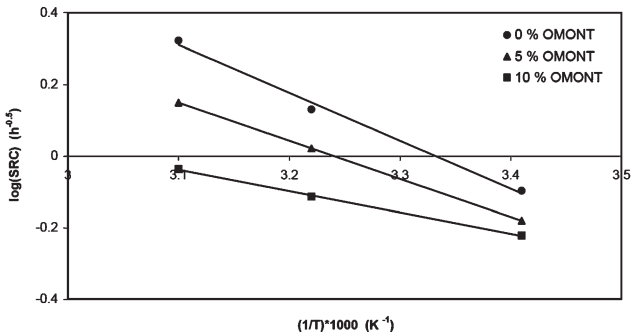

Figure 16 SRC curves versus swelling temperature for some typical hydrogels.

Arrhenius-type curve was prepared by plotting log (SRC) versus reciprocal absolute temperature ($1/T$) of swelling medium for any sample (Fig. 16). Reasonable linear curves were observed for pure and nanocomposite hydrogels between 20 and 50°C. Therefore, we may express the temperature dependent swelling characteristics of pure and nanocomposite PVA hydrogels (in the range of 20–50°C) by the following equation:

$$\log(\mathrm{SRC}) = c - \frac{d}{T} \tag{10}$$

where c and d are constants and similar to the constant values of a and b in eq. (9) they depend on the amounts and properties of the hydrogel components (PVA and OMONT) and also on the processing parameters. Parameters c and d can give us good measures of dependency of the swelling of nanocomposite hydrogels to the swelling medium temperature. For instance, c may be recognized as a measure of the maximum SRC of hydrogels in temperature range which swelling experiments have been performed. On the other hand, d can clearly tell us about the intensity of dependence of the hydrogel swelling to the swelling medium temperature, in a manner which a hydrogel with higher value of d has stronger dependence to the swelling medium temperature. The values of the parameters c and d for some prepared samples have been listed in Table I. It can bee seen that increasing the amount of clay in nanocomposite hydrogels causes the value of d to decrease, which reveals of a less effect of temperature on the SRC of PVA nanocomposite

TABLE I
The Values of the Parameters c and d [in eq. (10)] for Some Typical Hydrogels

Sample	c ($h^{-0.5}$)	d ($h^{-0.5}$ K^{-1})
0% OMONT	4.46	1338
5% OMONT	3.44	1063
10% OMONT	1.81	596

hydrogels compared to the clay-free PVA hydrogel. This may be attributed to more rigid nature and less flexibility of the PVA chains in nanocomposite hydrogel because of interactions created between polymer chains and clay layers in comparison to the pure PVA hydrogel, which limit the movements of polymer chains and as a result restrict the action of network in absorption of swelling agent in reaction to the temperature variations.

CONCLUSIONS

From the obtained results, we conclude that the OMONT acts as an additional crosslinker in the network structure of PVA-OMONT nanocomposite hydrogels and drastically affects their structural and swelling characteristics. The results showed that the swelling ability of the PVA hydrogel would be decreased by incorporating of the OMONT into it. This is in accordance with the higher gel fraction and ν_e amounts and also lower values of $(\overline{M}_c)$ and ξ for PVA nanocomposite hydrogel in comparison with pure PVA hydrogel. Swelling kinetics studies showed that linear relations exist between degrees of swelling and square root of immersion time in early stages of swelling period for pure and all nanocomposite hydrogels. Thus, it can be deduced that diffusion is the main phenomena governing the swelling of PVA-ONOMT nanocomposite hydrogels in the early stages of swelling process. The swelling behavior of PVA nanocomposite hydrogels at measured swelling medium temperatures exhibited that the swelling characteristics of hydrogels at equilibrium condition including EDWS, EWC, and EDVS increase by increasing the temperature, while the required time to reach to the equilibrium state decreases. The results also showed that the linear proportionality of degree of swelling against the square root of immersion time is still valid for pure PVA and nanocomposite hydrogels at measured swelling temperatures. Based on the obtained swelling characteristics of the PVA-OMONT nanocomposite hydrogels, we can optimize the clay loading level in nanocomposite hydrogels and choose the best one to our desired application, specially in biomedical applications, where the performance of the nanocomposite hydrogel is mainly controlled by its swelling capability.

References

1. Qiu, Y.; Park, K. Adv Drug Deliv Rev 2001, 53, 321.
2. Pourjavadi, A.; Aghajani, V.; Ghasemzadeh, H. J Appl Polym Sci 2008, 109, 2648.
3. Guilherme, M. R.; Silva, R.; Girotto, E. M.; Rubira, A. F.; Muniz, E. C. Polymer 2003, 44, 4213.
4. Hegazy, E. S. A.; El-Aal, S. E. A.; Taleb, M. F. A.; Dessouki, A. M. J Appl Polym Sci 2004, 92, 2642.
5. Murakami, Y.; Maeda, M. Biomacromolecules 2005, 6, 2927.
6. Peattie, R. A.; Rieke, E. R.; Hewett, E. M.; Fisher, R. J.; Shu, X. Z.; Prestwich, G. D. Biomaterials 2006, 27, 1868.
7. Liu, K.; Li, Y.; Xu, F.; Zuo, Y.; Zhang, L.; Wang, H.; Liao, J. Mater Sci Eng C 2009, 29, 261.
8. Efron, N.; Morgan, P. B. Cont Lens Anterior Eye 2008, 31, 242.
9. Sirousazar, M.; Yari, M. Chin J Polym Sci 2010, 28, 573.
10. Sirousazar, M.; Kokabi, M.; Yari, M. Iran J Pharm Sci 2008, 4, 51.
11. Schmidt, J. J.; Rowley, J.; Kong, H. J. J Biomed Mater Res A 2008, 87, 1113.
12. Zhou, H. Y.; Chen, X. G.; Kong, M.; Liu, C. S. J Appl Polym Sci 2009, 112, 1509.
13. Weian, Z.; Wei, L.; Yue'e, F. Mater Lett 2005, 59, 2876.
14. Zhu, M.; Liu, Y.; Sun, B.; Zhang, W.; Liu, X.; Yu, H.; Zhang, Y.; Kuckling, D.; Adler, H. J. P. Macromol Rapid Commun 2006, 27, 1023.
15. Zhang, W.; Liu, Y.; Zhu, M.; Zhang, Y.; Liu, X.; Yu, H.; Jiang, Y.; Chen, Y.; Kuckling, D.; Adler, H. J. P. J Polym Sci A Polym Chem 2006, 44, 6640.
16. Kasgoz, H.; Durmus, A.; Kasgoz, A. Polym Adv Technol 2008, 19, 213.
17. Ma, J.; Zhang, L.; Fan, B.; Xu, Y.; Liang, B. J Polym Sci B Polym Phys 2008, 46, 1546.
18. Haraguchi, K.; Takehisa, T. Adv Mater 2002, 14, 1120.
19. Schexnailder, P.; Schmidt, G. Colloid Polym Sci 2009, 287, 1.
20. Haraguchi, K.; Taniguchi, S.; Takehisa, T. Chem Phys Chem 2005, 6, 238.
21. Liu, Y.; Zhu, M.; Liu, X.; Jiang, Y. M.; Ma, Y.; Qin, Z. Y.; Kuckling, D.; Adler, H. J. P. Macromol Symp 2007, 254, 353.
22. Abdurrahmanoglu, S.; Can, V.; Okay, O. J Appl Polym Sci 2008, 109, 3714.
23. Song, L.; Zhu, M.; Chen, Y.; Haraguchi, K. Macromol Chem Phys 2008, 209, 1564.
24. Haraguchi, K.; Takehisa, T.; Fan, S. Macromolecules 2002, 35, 10162.
25. Nie, J.; Du, B.; Oppermann, W. Macromolecules 2005, 38, 5729.
26. Lee, W. F.; Fu, Y. T. J Appl Polym Sci 2003, 89, 3652.
27. Sur, G. S.; Lyu, S. G.; Chang, J. H. J Ind Eng Chem 2003, 9, 58.
28. Zolfaghari, R.; Katbab, A. A.; Nabavizadeh, J.; Tabasi, R. Y.; Nejad, M. H. J Appl Polym Sci 2006, 100, 2096.
29. Al, E.; Guclu, G.; Iyim, T. B.; Emik, S.; Ozgumus, S. J Appl Polym Sci 2008, 109, 16.
30. Kasgoz, H.; Durmus, A. Polym Adv Technol 2008, 19, 838.
31. Lee, W. F.; Chen, Y. C. J Appl Polym Sci 2004, 94, 692.
32. Lee, W. F.; Chen, Y. C. J Appl Polym Sci 2005, 98, 1572.
33. Lee, W. F.; Lee, S. C. J Appl Polym Sci 2006, 100, 500.
34. Lee, W. F.; Chen, Y. C. J Appl Polym Sci 2004, 91, 2934.
35. Lee, W. F.; Tsao, K. T. J Appl Polym Sci 2006, 100, 3653.
36. Thomas, V.; Yallapu, M. M.; Sreedhar, B.; Bajpai, S. K. J Appl Polym Sci 2009, 111, 934.
37. Frimpong, R. A.; Fraser, S.; Hilt, J. Z. J Biomed Mater Res A 2007, 80, 1.
38. Kokabi, M.; Sirousazar, M.; Hassan, Z. M. Eur Polym Mater 2007, 43, 773.
39. Sirousazar, M.; Kokabi, M.; Hassan, Z. M. J Biomater Sci Polym Ed 2011, 22, 1023.
40. Ricciardi, R.; Auriemma, F.; De Rosa, C.; Laupretre, F. Macromolecules 2004, 37, 1921.
41. Hassan, C. M.; Ward, J. H.; Peppas, N. A. Polymer 2000, 41, 6729.
42. Miyazaki, S.; Karino, T.; Endo, H.; Haraguchi, K.; Shibayama, M. Macromolecules 2006, 39, 8112.
43. Can, V.; Abdurrahmanoglu, S.; Okay, O. Polymer 2007, 48, 5016.
44. Peppas, N. A.; Bures, P.; Leobandung, W.; Ichikawa, H. Eur J Pharm Biopharm 2000, 50, 27.
45. Flory, P. Principles of Polymer Chemistry, Twelfth Printing; Cornell University Press: Ithaca, 1983.
46. Urushizaki, F.; Yamaguchi, H.; Nakamura, K.; Numajiri, S.; Sugibayashi, K.; Morimoto, Y. Int J Pharm 1990, 58, 135.